Inorg. Chem. **2004**, *43*, 6699–6706

New Tetranuclear Cu(II) Complexes: Synthesis, Structure, and Magnetic Properties

Ramesh Kapoor,* Ashok Kataria, Paloth Venugopalan, and Pratibha Kapoor*

Department of Chemistry, Panjab University, Chandigarh-160014, India

Montserrat Corbella*

Departament de Química Inorgànica, Universitat de Barcelona, Martí i Franquès 1-11, E-08028 Barcelona, Spain

Montserrat Rodríguez,*,† Isabel Romero,† and Antoni Llobet*,†

Departament de Química, Universitat de Girona, Campus de Montilivi E-17071, Girona, Spain

Received January 28, 2004

The synthesis, structure, and magnetic properties of two new tetranuclear Cu(II) complexes containing *N*,*N*,*N*′,*N*′-tetraethylpyridine-2,6-dithiocarboxamide (S-dept) of formula $[Cu_2Cl_2(\mu\text{-S-dept})_2][Cu_2Cl_4(\mu\text{-Cl})_2]$ (**1**) and $[Cu_2(\mu\text{-Cl})_2(\text{S-dept})_2][CuCl_3(EtOH)]_2$ (**2**) are reported. Their X-ray crystal structures reveal that the complexes are composed of anionic and cationic dimers, that in both cases contain the metal centers which interact via Coulombic and/or hydrogen bonding interactions. In both cases, the Cu centers in the anionic moieties adopt a slightly distorted tetrahedral geometry whereas for the cationic moieties they adopt a square-pyramidal type of geometry. Magnetic susceptibility data show that compounds **1** and **2** present an overall antiferromagnetic behavior arising from the contribution of both anionic and cationic moieties. For **1**, the best fit obtained gave $J_1 = -2.62 \pm 0.19$ cm^{-1}, $J_2 = -19.54 \pm 0.47$ cm^{-1}, and $g_2 = 2.164 \pm 0.004$ cm^{-1} ($R = 8.28 \times 10^{-5}$) whereas for **2** it gave $J_1 = 4.48 \pm 2.73$ cm^{-1}, $g_1 = 2.20 \pm 0.03$, $J_2 = -11.26 \pm 2.01$ cm^{-1}, and $g_2 = 2.10 \pm 0.03$ ($R = 1.15 \times 10^{-4}$). The nature of the superexchange pathways in **1** and **2** is discussed on the basis of structural, magnetic, and molecular orbital considerations. Theoretical calculations are performed at the extended Hückel level in order to obtain their molecular orbitals and energies using their crystallographic data.

Introduction

The study of magnetic properties of transition metal complexes has attracted increasing attention over the latest decades, given their broad array of technological uses.[1] In particular, Cu(II) binuclear complexes are of special significance for their enormous structural versatility, which allows a wide assortment of superexchange pathways and, consequently, of nature and intensities in magnetic couplings.[2,3]

We describe here the synthesis, structure, and magnetic behavior of new trinuclear Cu(II) complexes containing the *N*,*N*,*N*′,*N*′-tetraethylpyridine-2,6-dithiocarboxamide (S-dept) chelating ligand:

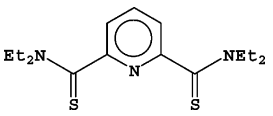

The described complexes show a variety of interaction pathways including Cl-bridge and the more uncommon S-bridge, as well as magnetic coupling via hydrogen bonding.

* To whom correspondence should be addressed. E-mail: montse.rodriguez@udg.es (M.R.); antoni.llobet@udg.es (A.L.); montse.corbella@ub.edu (M.C.); rkapoor@pu.ac.in (R.K.); pkapoor@pu.ac.in (P.K.).

† Departament de Química.

10.1021/ic049882j CCC: $27.50
Published on Web 09/17/2004

The nature of the superexchange interactions taking place is discussed on the basis of molecular orbitals calculations.

Experimental Section

Materials. All reactions were carried out in anhydrous solvents under dry N_2 atmosphere. Solvents were dried using standard techniques. Absolute ethanol (AR quality, Hayman Ltd.) and pyridine-2,6-dicarboxylic acid (Fluka) were used as supplied. Anhydrous $CuCl_2$ was prepared by boiling the hydrated salt under reflux with freshly distilled $SOCl_2$ for about 4 h. The anhydrous $CuCl_2$ was filtered, washed with dry benzene, and dried in vacuo.

***N,N,N′,N′*-Tetraethylpyridine-2,6-dithiocarboxamide (S-dept).** A mixture of diethylpyridine-2,6-dicarboxamide (DEAP)[4] (7.86 g, 0.028 mol) and P_2S_5 (3.93 g, 0.017 mol) was refluxed in benzene (40 mL) for 8 h. The reaction mixture was filtered to remove unreacted P_2S_5. Crude S-dept was obtained by removal of the solvent under vacuum. Pure S-dept was obtained as shining yellow crystals on crystallization from hot EtOH (yield: 6.80 g, 77%). Mp: 129−130 °C. Anal. Calcd for $C_{15}H_{23}N_3S_2$: C, 58.25; H, 7.44; N, 13.59%. Found: C, 58.17; H, 7.51; N, 13.52%. ^{1}H NMR ($CDCl_3$, TMS): $\delta = 7.5$ ppm (t, H3); 7.45 ppm (d, H4); 3.7 (q, H12); 1.29 (t, H13). The NMR assignment uses the same numbering scheme as that for the X-ray structure (see Figure 1). IR (KBr pellet, cm^{-1}): 1630 m, 1580 m, 1558 s, 1508 s, 1495 s, 1459 m, 1440 s, 1436 s, 1386 m, 1356 s, 1318 m, 1295 m, 1263 s, 1196 m, 1145 m, 1117 m, 1096 m, 1076 s, 990 m, 818 m, 776 m, 723 m, 690 m, 626 m, 558 m, 508 m, 457 m, 418 m.

$[Cu_2Cl_2(\mu$-S-dept$)_2][Cu_2Cl_4(\mu$-Cl$)_2]$ (1). A solution of anhydrous $CuCl_2$ (2.47 g, 0.018 mol) in acetonitrile (20 mL) was added dropwise to a magnetically stirred solution of S-dept (2.84 g, 0.009 mol) in acetonitrile (20 mL). The resulting solution was refluxed for 6 h. Upon cooling to room temperature, a dark green crystalline solid separated out. The solid was filtered, washed with ethanol (3 mL) and dry petroleum ether (2 × 5 mL), and dried in vacuo. Yield: 4.61 g, 87%. Mp: 146 °C. Anal. Found: C, 31.21; H, 4.31; N, 6.98; Cl, 24.1; S, 11.0. Calcd for $C_{30}H_{46}N_6S_4Cl_8Cu_4$: C, 31.14; H, 3.98; N, 7.26; Cl, 24.6; S, 11.1%. IR (KBr pellets, cm^{-1}): 1605 s, 1532 vs, 1426 m, 1314 m, 1275 m, 1254 w, 1172 s, 1152 m, 1072 m, 1020 m, 897 m, 810 m, 763 m, 683 m, 651 m, 509 m, 487 m, 443 m. Molar conductance ($\Omega^{-1}\cdot cm^2\cdot mol^{-1}$): 120 (MeOH) and 94 ($CH_3NO_2$). UV−vis [$\lambda_{max}$, nm ($\epsilon$, $M^{-1}\cdot cm^{-1}$)] in MeOH: 401 (158), 775 (393.5). In CH_2Cl_2: 401 (55), 661 (78.5), 796 (90).

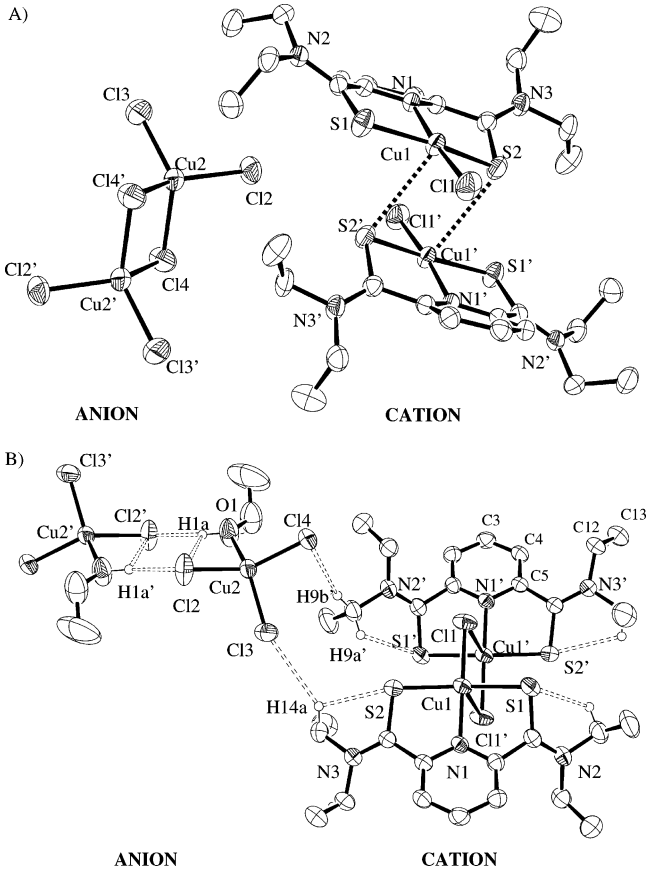

Figure 1. ORTEP views (ellipsoids at 50% probability) of the molecular structure of (A) $[Cu_2Cl_2(\mu$-S-dept$)_2][Cu_2Cl_4(\mu$-Cl$)_2]$ (**1**) and (B) $[Cu_2(\mu$-Cl$)_2$(S-dept$)_2][CuCl_3$(EtOH)$]_2$ (**2**).

$[Cu_2(\mu$-Cl$)_2$(S-dept$)_2][CuCl_3$(EtOH)$]_2$ (2). Compound **2** was prepared following exactly the same experimental procedure as that used for **1** but by using absolute ethanol as solvent. A dark green solid (yield: 4.76 g, 89%) was obtained. Mp: 191 °C. Anal. Found: C, 32.52; H, 4.50; N, 6.61. Calcd for $C_{34}H_{58}N_6S_4C_{28}O_2Cu_4$: C, 32.69; H, 4.64; N, 6.73%. IR (KBr pellets, cm^{-1}):1602 s, 1543 s, 1424 m, 1317 vs, 1282 m, 1259 m, 1187 m, 1098 m, 1072 m, 1022 m, 911 m, 897 s, 804 m, 758 m, 721 m, 651 s. Molar conductance ($\Omega^{-1}\cdot cm^2\cdot mol^{-1}$): 122 (MeOH) and 96 ($CH_3NO_2$). UV−vis [$\lambda_{max}$, nm ($\epsilon$, $M^{-1}\cdot cm^{-1}$)] in MeOH: 401 (581), 749 (530). In CH_2Cl_2: 400 (156), 662 (31.7), 794 (35.6).

Physical Methods. Elemental analyses (C, H, N) were performed on a Perkin-Elmer model 2400 CHN elemental analyzer. Chlorine was determined by Volhard's method,[5] and sulfur by precipitation as $BaSO_4$. IR spectra were recorded as KBr pellets on a Perkin-Elmer RX-I FTIR spectrophotometer. Molar conductances were measured using a Digital conductivity bridge, model CC601. The UV−vis spectra were recorded on a JASCO V-530 UV−Vis spectrophotometer. Magnetic susceptibilities were measured on polycrystalline powders at the Servei de Magnetoquímica of the Universitat de Barcelona with a Faraday type magnetometer (MANICS DSM8) equipped with an Oxford CF 1200 S helium continuous-flow cryostat working in the temperature range 4−300 K. Diamagnetic corrections were estimated from the Pascal Tables. EPR spectra were recorded at X-band (9.4 GHz) frequencies with a Bruker ESP-300E spectrometer, at 4 K.

(1) (a) Reedijk, J. In *Bioinorganic Catalysis*; Marcel Dekker: New York, 1993. (b) Carlin, R. L. In *Magnetochemistry*; Springer-Verlag: Berlin, 1986. (c) Solomon, E. I.; Wilcox, D. E. In *Magneto-structural correlations in exchange coupled systems*; Gatteschi, D., Kahn, O., Willett, R. D., Eds.; NATO Advanced Study Institute Series, Vol. C140; D. Reidel: Dordrecht, Holland, 1984. (d) Aromí, G.; Gamez, P.; Roubeau, O.; Kooijman, H.; Spek, A. L.; Diressen, W. L.; Reedijk, J. *Angew. Chem., Int. Ed.* **2002**, *41*, 1169−1170. (e) Cornia, A.; Gatteschi, D.; Sessoli, R. *Coord. Chem. Rev.* **200**1, *219*, 573−604. (f) Kahn, O. In *Modular Chemistry*; Michl, J., Ed.; Kluwer: Dordrecht, 1997; Vol. 499, pp 287−302.

(2) (a) Kapoor, P.; Pathak, A.; Kapoor, R.; Venugopalan, P.; Corbella, M.; Rodríguez, M.; Robles, J.; Llobet, A. *Inorg. Chem.* **2002**, *41*, 6153−6160. (b) Rodríguez, M.; Llobet, A.; Corbella, M. *Polyhedron* **2000**, *19*, 2483−2491. (c) Rodríguez, M.; Llobet, A.; Corbella, M.; Martell, A. E.; Reibenspies, J. *Inorg. Chem.* **1999**, *38*, 2328−2334.

(3) (a) Pardo, E.; Faus, J.; Julve, M.; Lloret, F.; Muñoz, M. C.; Cano, J.; Ottenwaelder, X.; Journaux, Y.; Carrasco, R.; Blay, G.; Fernandez, I.; Ruiz-García, R. *J. Am. Chem. Soc.* **2003**, *125*, 10770−10771. (b) Psomas, G.; Raptopoulou, C. P.; Iordanidis, L.; Dendrinou-Samara, C.; Tangoulis, V.; Kessissoglou, D. P. *Inorg. Chem.* **2000**, *39*, 3042−3048. (c) Ferlay, S.; Jouaiti, A.; Loi, M.; Hosseini, M. W.; De Cian, A.; Turek, P. *New J. Chem.* **2003**, 1801−1805. (d) Cano, J.; Ruiz, E.; Alemany, P.; Lloret, F.; Alvarez, S. *J. Chem. Soc., Dalton Trans.* **1999**, 1669−1676.

(4) Kapoor, P.; Kumar, A.; Nistandra, J.; Venugopalan, P. *Transition Met. Chem.* **2000**, *25*, 465−469.

(5) Volhard, J. *J. Prakt. Chem.* **1874**, *117*, 217.

Table 1. Crystallographic Data for Compounds **1** and **2**

	compound **1**	compound **2**
empirical formula	$C_{30}H_{46}Cl_8Cu_4N_6S_4$	$C_{34}H_{58}Cl_8Cu_4N_6O_2S_4$
fw	578.36	624.43
cryst syst	triclinic	triclinic
space group	$P\bar{1}$	$P\bar{1}$
a, Å	8.157(1)	8.925(1)
b, Å	10.002(1)	12.713(1)
c, Å	13.970(1)	13.025(1)
α, deg	78.00(1)	72.21(1)
β, deg	85.86(1)	89.11(1)
γ, deg	87.16(1)	87.21(1)
V, Å^3	1111.25(19)	1306.3(1)
Z	2	2
T, K	293(2)	293
λ(Mo Kα), Å	0.71073	0.71073
ρ_{calcd}, g/cm^3	1.729	1.552
μ, mm^{-1}	2.588	2.211
R_1[a]	0.0255	0.0268
wR_2[b]	0.0636	0.0691
	($m = 0.0242$, $n = 0.8665$)	($m = 0.0288$, $n = 0.8385$)

[a] $R_1 = \sum||F_o| - |F_c||/\sum|F_o|$. [b] $wR_2 = [\sum\{w(F_o^2 - F_c^2)^2\}/\sum\{w(F_o^2)^2\}]^{1/2}$, where $w = 1/[\sigma^2(F_o^2) + (mP)^2 + (nP)]$ and $P = (F_o^2 + 2F_c^2)/3$.

X-ray Crystallography. For compound **1**, intensity data were collected on a Siemens P4 single-crystal diffractometer equipped with a molybdenum sealed tube ($\lambda = 0.71073$ Å) and highly oriented graphite monochromator using crystals of dimensions 0.29 × 0.24 × 0.20 mm^3 and mounted in Lindeman glass capillaries. The lattice parameters and standard deviations were obtained by least-squares fit to 40 reflections ($9.53° < 2\theta < 29.97°$). The data were collected by the $2\theta-\theta$ scan mode with a variable scan speed ranging from 2.0°·min^{-1} to a maximum of 60.0°·min^{-1}. Three reflections were used to monitor the stability and orientation of the crystal and were measured after every 97 reflections. Their intensities showed only statistical fluctuations during 38.89 h of X-ray response time. The data were collected for Lorentz and polarization factors and on empirical absorption correction based on the ψ-scan method applied.

The structure was solved by the direct methods using SHELX-97[6] and also refined on F^2 using the same. All the non-hydrogen atoms were refined anisotropically. The hydrogen atoms were included in the ideal positions with fixed isotropic *U* values and were riding with their respective non-hydrogen atoms. A weighting scheme of the form $w = 1/[(\sigma^2F_o^2) + (aP)^2 + bP]$ with $a = 0.0242$ and $b = 0.87$ was used. The refinement converged to a final *R* value of 0.0255 (wR2 = 0.0636 for 3185 reflections) [$I > 2\sigma(I)$]. The final difference map was featureless. Neutral atom scattering factors and anomalous scattering correction terms were taken from the International Tables for X-ray Crystallography.[7]

The data collection procedure, structure solution, and refinement for compound **2** were essentially the same as those for **1**. The parameters associated with the structures are as follows: 40 reflections ($9.69° < 2\theta < 32.83°$) for an accurate cell parameter determination, 0.26 × 0.25 × 0.15 mm^3 crystal, a total of 42.24 h of X-ray exposure time, $R = 0.0268$ (wR2 = 0.0691 for 3689 reflections) [$I > 2\sigma(I)$] with $a = 0.0288$ and $b = 0.84$ in the weighting scheme. Full details are presented in Table 1.

Calculations. Molecular orbital calculations were carried out using CACAO (*Computer Aided Composition of Atomic Orbitals*, PC Beta-Version 5.0, 1998),[8] a program based on extended Hückel type of analysis using crystallographic coordinates.

Table 2. Selected Bond Distances (Å) and Angles (deg) for Compounds **1** and **2**

compound **1**		compound **2**	
Cu1−N1	1.991(2)	Cu1−N1	1.978(2)
Cu1−S1	2.2505(8)	Cu1−Cl1	2.2306(8)
Cu1−S2	2.2795(8)	Cu1−S2	2.2680(8)
Cu1−Cl1	2.2098	Cu1−S1	2.3248(8)
Cu1−S2′	3.419	Cu1−Cl1′	2.814
Cu1−Cu1′	4.166	Cu1−Cu1′	3.412
Cu2−Cl3	2.1824(9)	Cu2−O1	2.019(2)
Cu2−Cl2	2.1937(8)	Cu2−Cl3	2.1946(9)
Cu2−Cl4	2.3086(9)	Cu2−Cl4	2.2075(8)
Cu2−Cl4′	2.3230(9)	Cu2−Cl2	2.2345(9)
Cu2−Cu2′	3.304	Cu2−Cu2′	5.94
		Cl2−H1a′	2.232
N1−Cu1−Cl1	173.22(6)	N1−Cu1−Cl1	179.31(6)
S1−Cu1−S2	169.85(3)	S1−Cu1−S2	158.32(3)
N1−Cu1−S1	86.12(6)	N1−Cu1−S1	86.98(6)
Cl1−Cu1−S1	93.62(3)	Cl1−Cu1−S1	93.47(3)
N1−Cu1−S2	87.11(6)	N1−Cu1−S2	85.37(6)
Cl1−Cu1−S2	93.98(3)	Cl1−Cu1−S2	94.39(3)
S2−Cu1−S2′	88.28	Cl1−Cu1−Cl1′	95.71
Cu1−S2−Cu1′	91.72	Cu1−Cl1−Cu1′	84.29
Cl3−Cu2−Cl2	104.18(4)	Cl3−Cu2−Cl4	99.90(3)
Cl3−Cu2−Cl4	132.75(4)	Cl4−Cu2−Cl2	141.22(4)
Cl2−Cu2−Cl4	100.02(3)	Cl3−Cu2−Cl2	101.50(4)
Cl4−Cu2−Cl4′	88.98(3)	O1−Cu2−Cl3	138.39(9)
Cu2−Cl4−Cu2′	91.02(3)	O1−Cu2−Cl2	89.52(7)
		Cu2−O1−Cu2′	112.8

Results and Discussion

Synthesis and Structure. Compounds **1** and **2** were obtained in good yield by refluxing anhydrous $CuCl_2$ and the S-dept ligand (molar ratio 2:1) in an acetonitrile or absolute ethanol solution respectively, as shown in the eq 1 for compound **1**.

$$2CuCl_2 + \text{S-dept} \xrightarrow[\text{reflux}]{CH_3CN} \underset{\mathbf{1}}{[Cu_2Cl_2(\mu\text{-S-dept})_2][Cu_2Cl_4(\mu\text{-Cl})_2]} \quad (1)$$

Both compounds are air and moisture stable and were identified and characterized through melting points and elemental analyses, IR data, conductivity measurements, X-ray crystallography, and magnetic measurements. The compounds readily dissolve in polar organic solvents such as CH_3OH, C_2H_5OH, CH_3CN, CH_3NO_2, or $C_6H_5NO_2$. The conductivities of **1** and **2** were measured in MeOH and $MeNO_2$ at different concentrations and are typical of 1:1 electrolytes in reasonable agreement with literature data.[9]

Crystallization of $[Cu_2Cl_2(\mu\text{-S-dept})_2][Cu_2Cl_4(\mu\text{-Cl})_2]$, **1**, by slow evaporation of its saturated solution in acetonitrile at room temperature yields good single crystals. The corresponding crystallographic data and selected structural parameters are shown in Tables 1 and 2, respectively. The crystal structure for compound **1** is depicted in Figure 1A. The compound contains a cationic binuclear unit, $[Cu_2Cl_2(\mu\text{-S-dept})_2]^{2+}$, and an anionic dimer with formula $[Cu_2Cl_4(\mu\text{-Cl})_2]^{2-}$. It is noticeable here that the cationic fragment

(6) Sheldrick, G. M. *SHELX-97, Program for the Solution and Refinement of Crystal Structures*; University of Göttingen: Göttingen, Germany, 1997.
(7) *International Tables for X-ray Crystallography*; Wilson, A. J. C., Ed.; Kluwer Academic Publishers: Dordrecht, 1992; Vol. C, pp 500−502, 219−222, and 193−199.
(8) Mealli, C.; Proserpio, D. M.; Ienco, A. *J. Chem. Educ.* **1990**, *67*, 399−402.
(9) Geary, W. J. *Coord. Chem. Rev.* **1971**, *7*, 81−122.

Scheme 1. Twisting Angle

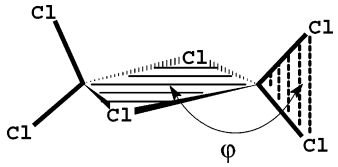

presents a very unusual Cu···Cu disposition taking place through bridging sulfur atoms, found only in a small number of Cu(II) complexes.[10,11] The coordination geometry around each metal center is vaguely distorted square pyramidal (Reedijk's τ factor[12] is 0.05, denoting an almost regular pyramidal geometry), where the basal plane is defined by the pyridylic N atom and the two S atoms of the S-dept ligand, and also by a terminal chloro ligand. The apical position of the square pyramid is occupied by one of thesulfur atoms coordinated to the second Cu metal center, acting as bridging ligand.

Coordination of the S-dept ligand to the Cu metal center can a priori take place either through its sulfur or amide nitrogen atoms of the structure. Electronic factors, as outlined in Pearson's theory,[13] would predict, for a Cu(II) complex, the N−N−N mode of coordination to the metal center. Then, the S−N−S set of coordinative atoms found in S-dept seems to be governed mainly by steric factors, the latter interaction mode being the most favored as is also the case in the structures of related compounds.[2a,4]

The relative arrangement of both square pyramids, sharing a basal-to-apical edge, places the corresponding basal planes in a parallel position. The $Cu_2(\mu\text{-}S)_2$ core is rectangular, with a Cu−(μ-S)−Cu angle of 91.72°, a Cu−S_{basal} bond distance of 2.279 Å, and just a contact for the apical position, with a distance Cu···S_{apical} of 3.419 Å. Given this contact and the weak magnetic interaction (see the following section) found between these two units, we will refer to them from now on as a pseudodimer.

The anionic fragment in compound **1**, $[Cu_2Cl_4(\mu\text{-}Cl)_2]^{2-}$, consists of two tetracoordinated Cu metal centers bridged by two chloro ligands. The coordination environment of each Cu atom is completed with two terminal Cl ligands, determining a tetrahedrally distorted geometry around the metal. The $Cu_2(\mu\text{-}Cl)_2$ core is rightly planar and presents a Cu···Cu distance of 3.304 Å, and a Cu−(μ-Cl)−Cu angle of 91.02°. For Cu_2Cl_6 structures, a twist angle φ can be defined (see Scheme 1), which is the angle found between the plane defined by the Cu metal center and its two terminal chloro ligands, and the core plane. A value $\varphi = 0°$ states a completely planar dimer, whereas $\varphi = 90°$ would correspond to a perfect tetrahedral environment around the Cu metal center. The φ values found up to now in the literature range from 0°[14] to around 59°,[15] even though the most usual values are found around 45°−50°.[16] The anionic moiety in compound **1** presents the highest φ angle described to date for this class of Cu_2Cl_6 species, taking a value of 63.05°. The particular structure of compound **1** prompted us to study its magnetic properties in order to compare them with those of structurally similar compounds.

Compound **2** was obtained following a similar procedure to the one depicted in eq 1 for the synthesis of **1**, but by using absolute ethanol as solvent. The structure of **2**, obtained after recrystallization in ethanol, is presented in Figure 1B. Tables 1 and 2 summarize crystallographic and structural data.

The structure of compound **2** consists of a cationic binuclear moiety, $[Cu_2(\mu\text{-}Cl)_2(S\text{-}dept)_2]^{2+}$, and two close anionic species with formula $[CuCl_3(EtOH)]^-$, conforming a pseudodinuclear unit. In the cationic fragment, each copper atom is pentacoordinated by the pyridilic N atom and the two S atoms of the S-dept ligand, as well as by two chloro ligands acting in a bridging mode. Each metal center presents a distorted square pyramidal geometry (Reedijk's τ factor for the distinction between square planar and bipyramidal geometry[12] takes a value of 0.35). Both square pyramids in the dimeric unit share a basal-to-apical edge in such a way that the corresponding basal planes are disposed in a parallel fashion and are related by a C_2 symmetry axis, with a Cu···Cu distance of 3.412 Å. The $Cu_2(\mu\text{-}Cl)_2$ core in the binuclear unit is perfectly planar and presents a slightly distorted rectangular shape (Cu−Cl bond distances are 2.231 and 2.814 Å for the basal and the apical positions, respectively, whereas the Cu−Cl−Cu angle is 84.29°). The bond distances and angles are within the usual range for this type of compound.[17,18,19b]

(10) Garcia-Tojal, J.; Urtiaga, M. K.; Cortes, R.; Lezama, L.; Arriortua, M. I.; Rojo, T. *J. Chem. Soc., Dalton Trans.* **1994**, 2233−2238.
(11) (a) Jian, F. F.; Wang, Z.; Bai, A.; You, X.; Fun, H.-K.; Chinnakali, K.; Razak, R. A. *Polyhedron* **1999**, *18*, 3401−3406. (b) García-Tojal, J.; Lezama, L.; Pizarro, J. L.; Insausti, M.; Arriortua, M. I.; Rojo, T. *Polyhedron* **1999**, *18*, 3703−3711. (c) Fujisawa, K.; Moro-oka, Y.; Kitajima, N. *Chem. Commun.* **1994**, 623−624. (d) Branscombe, N. D. J.; Blake, A. J.; Marín-Becerra, A.; Li, W.-S.; Parsons, S.; Ruiz-Ramírez, L.; Schroder, M. *Chem. Commun.* **1996**, 2573−2574. (e) Gómez-Saiz, P.; García-Tojal, J.; Maestro, M. A.; Arnaiz, F. J.; Rojo, T. *Inorg. Chem.* **2002**, *41*, 1345−1347. (f) Houser, R. P.; Halfen, J. A.; Blackburn, N. J.; Tolman, W. B. *J. Am. Chem. Soc.* **1995**, *117*, 10745−10746.
(12) Addison, A. W.; Rao, T. N.; Reedijk, J.; Rijn, J. V.; Verschoor, G. C. *J. Chem. Soc., Dalton Trans.* **1984**, 1349−1356.
(13) Cowan, J. A. In *Inorganic Biochemistry: an introduction*; VCH Publishers: New York, 1993.
(14) (a) Nather, C.; Jess, I.; Bolte, M. *Acta Crystallogr., Sect. E* **2001**, *57*, m78. (b) Manfredini, T.; Pellacani, G. C.; Bonamartini-Corradi, A.; Battaglia, L. P.; Guarini, G. G. T.; Giusti, J. G.; Pon, G.; Willett, R. D.; West, D. X. *Inorg. Chem.* **1990**, *29*, 2221−2228. (c) Hasselgren, C.; Jagner, S.; Dance, I. *Chem.—Eur. J.* **2002**, *8*, 1269−1278.
(15) Fenske, D.; Goesmann, H.; Ernst, T.; Dehnicke, K. *Z. Naturforsch., B: Chem. Sci.* **1990**, *45*, 101.
(16) (a) Gatteschi, D.; Goslar, J.; Hilczer, W.; Hoffmann, S. K.; Zanchini, C. *Inorg. Chem.* **1996**, *35*, 1148−1153. (b) Kivikoski, J.; Fernandez, V.; Howard, J. A. K.; Hartung, J. *Acta Crystallogr., Sect. C* **1994**, *50*, 1886−1888. (c) Bencini, A.; Gatteschi, D.; Zanchini, C. *Inorg. Chem.* **1985**, *24*, 704−708.
(17) (a) Brown, S. J.; Tao, X.; Wark, T. A.; Stephan, D. W.; Mascharak, P. K. *Inorg. Chem.* **1988**, *27*, 1581−1587. (b) Rojo, T.; Arriortua, M. I.; Ruiz, J.; Darriet, J.; Villeneuve, D.; Beltran-Porter, J. *J. Chem. Soc., Dalton Trans.* **1987**, 285−291.
(18) (a) Lucas, C. R.; Liu, S.; Thompson, L. K. *Inorg. Chem.* **1990**, *29*, 85−88. (b) Tosik, A.; Maniukievicz, W.; Bukowska-Strzyzewska, M.; Mrozinski, J.; Sigalas, M. P.; Tsipis, C. A. *Inorg. Chim. Acta* **1991**, *190*, 193−203. (c) Kwiatkowski, E.; Kwiatkowski, M.; Olechnowicz, A.; Mrozinski, J.; Ho, D. M.; Deutsch, E. *Inorg. Chim. Acta* **1989**, *158*, 37−42.
(19) (a) Hay, P. J.; Thibeault, J. C.; Hoffmann, R. *J. Am. Chem. Soc.* **1975**, *97*, 4884−4899. (b) Roundhill, S. G. N.; Roundhill, D. M.; Bloomquist, D. R.; Landee, C.; Willett, R. D.; Dooley, D. M.; Gray, H. B. *Inorg. Chem.* **1979**, *18*, 831−835.

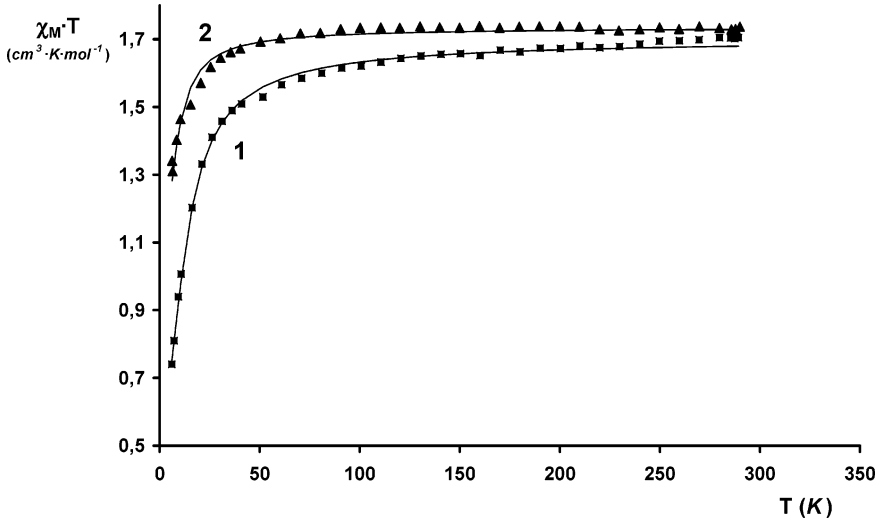

Figure 2. $\chi_M \cdot T$ vs T experimental data for **1** (■) and **2** (▲) (cm^3 K mol^{-1}). The solid lines show the best fits obtained (see text).

Each of the anionic fragments in **2** consists of a Cu metal center coordinated by three chloro ligands and the oxygen atom of an ethanol molecule. The geometry around the Cu atom generates a distorted tetrahedron, with Cl2−Cu2−Cl4 and Cl3−Cu2−O1 angles of 141.22° and 138.38°, respectively.

The arrangement of the different species present in the lattice structure allows a certain degree of H-bond interaction throughout the crystal, thus generating a one-dimensional system (see Figure 1B). On one hand, within the pseudodinuclear anion, two neighboring $[CuCl_3(EtOH)]^-$ entities present a double interaction between two chloro ligands and the H atoms directly bonded to the O atoms of the ethanol molecules (d(Cl−H) = 2.232 Å, d(O−H) = 0.924 Å, d(O···Cl) = 3.103 Å, ∠Cl−H−O = 156.89°). The two Cu metal centers are placed 5.94 Å away from each other. The bond distance between the Cu and the Cl involved in H-bonding (2.235 Å) is somewhat higher than the corresponding Cu−Cl(terminal) bond distances, which are 2.207 and 2.195 Å, respectively. On the other hand, one of the anionic $[CuCl_3(EtOH)]^-$ units presents an additional H-bond interaction with the cationic dimer through its Cl3 and Cl4 atoms, with bond distances Cl4−H9b = 2.932 Å and Cl3−H14a = 2.991 Å. There are also intramolecular interactions within the dimeric cation involving sulfur atoms (H9a−S1 = 2.685 Å, H14a−S2 = 2.541 Å).

Magnetic Properties. Figure 2 shows a plot of $\chi_M \cdot T$ versus T for compounds **1** and **2** (solid lines show the best fit obtained, vide infra). At room temperature, both compounds present a $\chi_M \cdot T$ value of approximately 1.7 $cm^3 \cdot K \cdot mol^{-1}$, in agreement with the presence of four Cu(II) metal centers per mole of compound. Upon decreasing the temperature, $\chi_M \cdot T$ for compound **1** varies scarcely until T = 70 K, where it dramatically drops off to a value of 0.743 $cm^3 \cdot K \cdot mol^{-1}$ at 5.99 K, thus manifesting an overall antiferromagnetic coupling. Compound **2** behaves in a similar manner, withan important decrease of $\chi_M \cdot T$ at T below 50 K reaching a value of $\chi_M \cdot T$ = 1.31 $cm^3 \cdot K \cdot mol^{-1}$ at 6.43 K.

Bearing in mind the nature of compounds **1** and **2**, two different approaches can be considered to fit magnetic data. As illustrated previously in the structural description, the compounds can be regarded (1) as formed by a dimeric complex unit together with two monomeric counterions or (2) as constituted by two binuclear entities. The corresponding data fits have been performed in view of both scenarios.

Thus, in a first approach for compound **1**, the cationic $[Cu_2Cl_2(\mu\text{-S-dept})_2]^{2+}$ unit was considered as two magnetically independent monomers, given the long Cu−(μ-S) distance found (3.419 Å), and hence, the magnetic interaction would arise only from the anionic $[Cu_2Cl_4(\mu\text{-Cl})_2]^{2-}$ moiety. The experimental data were taken as the sum of the $\chi_M \cdot T$ values of the binuclear complex and of two $[CuCl(S\text{-dept})]^+$ monomeric entities. The spin Hamiltonian considered was $H = -J \cdot S_1 \cdot S_2$, and the expression of $\chi_M \cdot T$ is represented by the following Bleaney−Bowers equation.

$$\chi_M \cdot T = [N g_d^2 \beta^2 2/k(1 + 3 \exp(J/kT)] + 2[N g_m^2 \beta^2/4k] \quad (2)$$

The data fitting was optimized by minimizing the function $R = \Sigma(\chi_M T_{calc} - \chi_M T_{obs})^2/\Sigma(\chi_M T_{obs})^2$, and the best values obtained were $J = -19.19 \pm 0.59$ cm^{-1}, $g_d = 2.25 \pm 0.02$, $g_m = 2.00 \pm 0.02$ ($R = 1.2 \times 10^{-4}$). However, experimental $\chi_M T$ data at low temperatures exhibited slightly inferior values than those expected from the theoretical fit performed in this way (for instance, $\chi_M T$ at 5.99 K is 0.7431 $cm^3 \cdot K \cdot mol^{-1}$ whereas the calculated value is 0.7847 $cm^3 \cdot K \cdot mol^{-1}$), indicating the presence of weak additional antiferromagnetic interactions probably assignable to a minor interaction between the cationic units.

The data fitting was then performed by means of eq 3, which was obtained using the following Bleaney−Bowers equation also based on the spin Hamiltonian $H = -J \cdot S_1 \cdot S_2$, and that allows for the two contributions mentioned: one arising from the superexchange interaction within the dimeric anionic complex and another one from the two $[CuCl(S\text{-dept})]^+$ units bridged through the S atoms of the S-dept ligand ($\chi_M \cdot T = (\chi_M \cdot T)_{dimer1} + (\chi_M \cdot T)_{dimer2}$).

$$\chi_M T = [N g_1^2 \beta^2 2/k(1 + 3 \exp(J_1/KT)] + [N g_2^2 \beta^2 2/k(1 + 3 \exp(J_2/kT)] \quad (3)$$

The g value for the cationic complex was fixed at $g_1 = 2.1$ (value obtained from ESR experiments, see a following section). The best fit was obtained with $J_1 = -2.62 \pm 0.19$ cm^{-1}, $J_2 = -19.54 \pm 0.47$ cm^{-1}, and $g_2 = 2.164 \pm 0.004$ cm^{-1} ($R = 8.28 \times 10^{-5}$), which represents an improved fit for compound **1** data.

In the case of compound **2**, we could consider similar approaches to those used for compound **1** to fit magnetic data. The best J values obtained following the first approach described (eq 1, meaning in this case a dimeric $[Cu_2(\mu\text{-Cl})_2(\text{S-dept})_2]^{2+}$ unit and two $[CuCl_3(EtOH)]^-$ monomers) gave a value of $J = -7.66 \pm 3.13$ cm^{-1}, $g_d = 2.10 \pm 0.43$, and $g_m = 2.20 \pm 0.41$, with $R = 1.32 \times 10^{-4}$. On the other hand, the second approach tested, which takes into consideration an additional exchange pathway going on through hydrogen bonding between two neighboring $[CuCl_3(EtOH)]^-$ units (eq 3, two binuclear units), brings to a value of $J_1 = 4.48 \pm 2.73$ cm^{-1}, $g_1 = 2.20 \pm 0.03$, $J_2 = -11.26 \pm 2.01$ cm^{-1}, and $g_2 = 2.10 \pm 0.03$ ($R = 1.15 \times 10^{-4}$).

The assignment of the different coupling constants J_1 and J_2 to one or another dimeric unit in each compound is done from comparison with analogous systems as well as by taking into account structural parameters and molecular orbitals calculations.

First, as stated in the preceding structural discussion for compounds **1** and **2**, the geometry within the respective cationic units, $[Cu_2Cl_2(\mu\text{-S-dept})_2]^{2+}$ for compound **1** and $[Cu_2(\mu\text{-Cl})_2(\text{S-dept})_2]^{2+}$ for **2**, disposes the corresponding magnetic planes (bases of the square pyramids) in a parallel fashion. Comparison with structurally related dimers would predict, for these cationic moieties, a practically negligible magnetic coupling that is either ferro- or antiferromagnetic, given the fact that this arrangement usually leads to little or null interaction as the effective orbital overlap is close to zero throughout the bridge.[2b] A small magnetic coupling is then expected from these units, and therefore, the lower coupling constants calculated for each compound are assigned to the magnetic interaction taking place within their respective cationic moieties ($J_{C1} = -2.62$ cm^{-1}, $J_{C2} = 4.48$ cm^{-1}, where J_{C1} and J_{C2} stand for the coupling constants corresponding to the cationic moieties of compounds **1** and **2**, respectively). Conversely, the larger J values are assigned to the related anionic fragments, which are discussed in the following.

The Cu_2Cl_6 anionic unit in compound **1** belongs to a well-known family of binuclear copper complexes. Magneto-structural correlations described for $Cu_2(\mu\text{-Cl})_2$ dimers establish, similarly to the $Cu_2(\mu\text{-OH})_2$ complexes, a linear relationship between singlet−triplet energy separation and the bridging angle α (see Figure 3).[19] However, this correlation is strictly applicable only to planar dimers (coplanar magnetic planes), since it is not possible to correlate magnetic properties between compounds having different coordination polyhedra.[2b,c] Geometrical deviations from planarity ($\varphi \neq 0$, as in **1**) lead to deviations from the correlation that are not completely understood. In this sense, compound **1** represents an exceptionally good element since

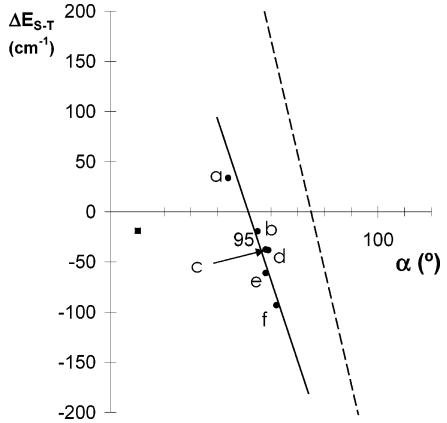

Figure 3. Magneto-structural correlation diagram for binuclear complexes of the type $Cu_2(\mu\text{-Cl})_2$ (—) and $Cu_2(\mu\text{-OH})_2$ (- - -).[2b] The circles (●) represent some planar Cu_2Cl_6 complexes (see ref 28), and the square (■) corresponds to the anionic complex in compound **1**.

it presents the highest φ angle found within this group of compounds.

The mentioned linear relationship between ΔE_{S-T} (energy difference between singlet and triplet states) and the bridging angle α for bis-μ-chloro copper(II) complexes, presented in Figure 3, would predict a large ferromagnetic coupling (with ΔE_{S-T} values higher than 200 cm^{-1}) for the anionic entity of compound **1**. However, the high value of φ found (and the consequent pseudotetrahedral geometry around each metal center) brings the anionic complex geometry far from planarity, dramatically influencing the magnetic interaction by deviating it from the expected value. The occurrence of a φ angle different from zero was thought to be responsible for an experimental deviation toward the antiferromagnetism with respect to the linear correlation.[20] However, theoretical studies[19a,21] performed on Cu_2Cl_6 dimers upon changing the φ angle for a given bridging angle α predict an important antiferromagnetic contribution to the coupling constant for $\varphi = 0°$ (planar dimers) and also for high φ values ($\varphi = 70-90°$), whereas for φ angles close to 45° the magnetic interaction would be ferromagnetic. From these studies, a very strong antiferromagnetic coupling would be expected for the anionic fragment of compound **1**, which is not actually found experimentally (the coupling constant for this interaction, J_{A1}, takes a value of around −19 cm^{-1}). This can be explained because the coupling constant established is in fact a sum of two opposite contributions: a ferromagnetic one, related to the exchange integral K_{ab},[22] and expected for the relatively small angle α of 91.02° (see Figure 3), and an antiferromagnetic one, coming from the high φ value found in the complex structure, then resulting in a medium intensity antiferromagnetic global interaction.

(20) (a) Willett, R. D.; Chow, C. *Acta Crystallogr., Sect. B* **1974**, *30*, 207. (b) Textor, M.; Dubler, E.; Oswald, R. *Inorg. Chem.* **1974**, *13*, 1361−1365.

(21) (a) Castell, A.; Miralles, J.; Caballol, R. *Chem. Phys.* **1994**, *179*, 377−384. (b) Bencini, A.; Gatteschi, D. *J. Am. Chem. Soc.* **1986**, *108*, 5763−5771. (c) Broer, R.; Maaskant, W. J. A. *Chem. Phys.* **1986**, *102*, 103.

(22) (a) Kahn, O. *Inorg. Chim. Acta* **1982**, *62*, 3−14. (b) Kahn, O. *Angew. Chem., Int. Ed. Engl.* **1985**, *24*, 834−850.

For compound **2**, the overall magnetic coupling throughout the compound is weakly antiferromagnetic in nature, with a J value around -11 cm^{-1}. It is not obvious whether this coupling is due primarily to a superexchange pathway taking place through the chloro bridges in the cationic moiety (first approach described), or if it is due to the hydrogen bonding between monomeric anions (second approach), since a good fit is obtained regardless of the approach utilized. However, hydrogen bonding has been shown[23] to effectively propagate exchange interactions of varying strengths (depending on the coplanarity of the magnetic orbitals), ranging from weak to strong antiferromagnetic coupling. On the other hand, the cationic moiety is subjected to undergo some magnetic interaction even though its parallel bases geometry, since structural deviations from the ideal coordination environment (for instance the Cu$-(\mu$-Cl$)-$Cu angle of 84.29°, which represents one of the smallest found in the literature for this type of complexes) allow a certain degree of overlapping and therefore a J_{C2} different from zero can be established. Hence, the second approach used, which assigns a certain degree of magnetic interaction to both the cationic and anionic moieties of compound **2**, represents a reasonable interpretation of its magnetic behavior. The strength of the magnetic interaction is discussed next on the basis of molecular orbitals calculations.

Molecular Orbitals. With the aim to further evaluate the influence of the structure on the superexchange pathway for the compounds described, we have performed a series of extended Hückel calculations based on crystallographic coordinates. For the cationic moieties of both compounds, the frontier molecular orbitals obtained are similar to the ones reported for structurally related complexes,[2b,c,10,24] with a bridging ligand that presents an effective overlap only with one of the Cu metal centers, then indicating a poor overlap through the bridge (see Figure S1 in the Supporting Information for HOMO and LUMO orbitals drawings as well as for the corresponding overlap population values). On the other hand, the HOMO$-$LUMO energy gap is very small in both cases (0.073 eV for compound **1** and 0.011 eV for compound **2**). As a consequence, both ferromagnetic[22] and antiferromagnetic[19a] contributions to the coupling constant will probably be rather small for any of the cationic species, as is confirmed experimentally.

For the anionic species, the theoretical molecular orbitals obtained for compounds **1** and **2** are shown in Figure 4A,B, respectively. For compound **1**, the Cu metal centers present a pseudotetrahedral coordination geometry, and the hybrid orbitals located in the chloro bridging ligands allow a simultaneous interaction with both metal centers and thus a superexchange pathway between them. This entails a nonzero value of the exchange integral K_{ab}, bringing a certain ferromagnetic contribution to the coupling constant. However, the elevated φ angle of 63.05° induces an important energy splitting between HOMO and LUMO orbitals ($\Delta E_{\mathrm{HOMO-LUMO}} = 0.435$ eV), which otherwise would be nearly degenerate for the bridging angle of 91.02° presented by the complex.[19] This energy difference between frontier orbitals is directly related to the antiferromagnetic contribution to the coupling constant, which is far more important in magnitude than the ferromagnetic one, and thus, it is in agreement with the considerable antiferromagnetic coupling observed.

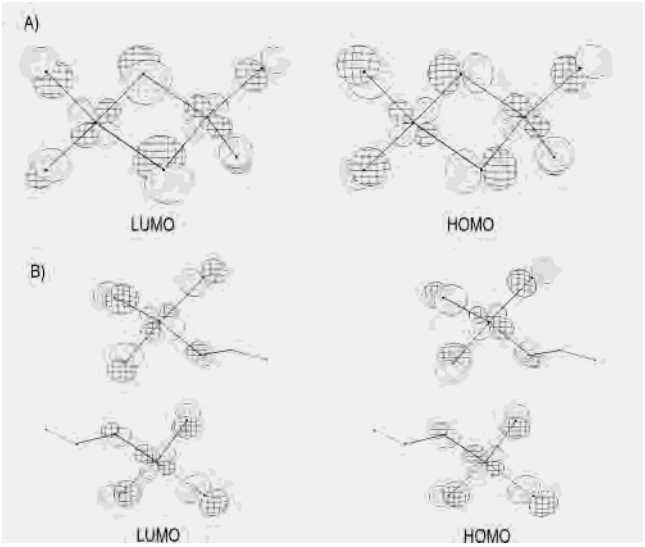

Figure 4. Drawings of SOMOs frontier orbitals (for orbitals contributing more than 1%) obtained for the anionic moieties of compounds **1** (A) and **2** (B).

Finally, it is noticeable here the difference that exists between the anionic counterion in **1** and the cationic moiety in **2**, despite the fact that both compounds belong to the Cu$_2$-(μ-Cl)$_2$ family of complexes; the dissimilar structural features that they present avoid a common magneto-structural correlation.

For **2**, the relative proximity of the metal centers between two neighboring [CuCl$_3$(EtOH)]$^-$ complex species allows a certain degree of interaction between the H atom of one ethanol molecule and a chloro ligand of a second one (overlap population H$-$Cl $= 0.046$), then permitting to some extent the magnetic coupling between metal centers. The role played by H-bonds in the superexchange phenomena is not completely understood and finds some handicaps in the accurate determination of the strength and nature of the interaction through this pathway, since many other intermolecular interactions usually compete in the solid state. For many years, H-bonds have been reported to propagate essentially antiferromagnetic interactions between metal centers in a variety of transition metal complexes,[25] even

(23) (a) Deplanches, C.; Ruiz, E.; Rodríguez-Fortea, A.; Álvarez, S. *J. Am. Chem. Soc.* **2002**, *124*, 5197−5205. (b) Ren, X. M.; Chen, Y. C.; He, C.; Gao, S. *J. Chem. Soc., Dalton Trans.* **2002**, 3915−3918. (c) Mohanta, S.; Lin, H. H.; Lee, C. J.; Wei, H. H. *Inorg. Chem. Commun.* **2002**, *5*, 585−588. (d) Yamada, Y.; Ueyama, N.; Okamura, T.-A.; Mori, W.; Nakamura, A. *Inorg. Chim. Acta* **1998**, 43−51. (e) Menon, S.; Balagopalakrishna, C.; Rajasekharan, M. V.; Ramakrishna, B. L. *Inorg. Chem.* **1994**, *33*, 950−954.

(24) (a) Marsh, W. E.; Hatfield, W. E.; Hodgson, D. J. *Inorg. Chem.* **1982**, *21*, 2679−2684. (b) Marsh, W. E.; Patel, K. C.; Hatfield, W. E.; Hodgson, D. J. *Inorg. Chem.* **1983**, *22*, 511.

(25) (a) Xie, Y.; Liu, Q.; Jiang, H.; Du, C.; Xu, X.; Yu, M.; Zhu, Y. *New J. Chem.* **2002**, *26*, 176−179 and references therein. (b) Paine, T. K.; Weyhermuller, T.; Wieghardt, K.; Chaudhuri, P. *Inorg. Chem.* **2002**, *41*, 6538−6540 and references therein.

though from theoretical studies the chance of ferromagnetic coupling should be considered.[26]

A recent theoretical study[23a] has been able to rationalize to some extent the antiferromagnetic coupling mediated by hydrogen bonds in Cu(II) complexes having square planar or square pyramidal geometry. For these geometries, it has been shown that the exchange interaction involves $d_{x^2-y^2}$-type orbitals of the metal centers, p-type orbitals of the ligands directly bonded to the metal, and s orbitals of the bridging H atoms. Then, the magnetic coupling can only take place through H atoms placed in equatorial positions of the corresponding pyramids, since in apical sites the effective overlap with the orbitals involved fades away. A similar effect goes on upon deviation of the coordination planes from coplanarity.[27] For compound **2**, however, the coordination environment around the Cu metal centers is pseudotetrahedral, and the atoms involved in the superexchange pathway (Cu−O−H−Cl−Cu) are not coplanar. This diminishes the symmetry of the corresponding hybrid orbitals (see Figure 4B for molecular orbitals drawings) and thus reduces to some extent the overlap throughout the bridge. This fact, together with the long Cu···Cu distance of 5.94 Å found, would foretell a relatively small coupling constant for the interaction between the two $[CuCl_3(EtOH)]^-$ anionic moieties, as is found experimentally.

EPR Spectra. Figure 5 displays the electron paramagnetic resonance (EPR) spectra registered for compounds **1** and **2** at 4 K. For compound **1**, two superimposed bands are found, at $g = 2.17$ and $g = 2.07$. Given the antiferromagnetic coupling constant of -19 cm^{-1} presented by the anionic Cu_2Cl_6 moiety, the EPR signal shown at 4 K must correspond to the cationic complex of compound **1**. Taking into account the weak Cu···Cu interaction occurring through the sulfur ligand bridges within the cationic moiety, the band at $g = 2.17$ could be assigned to $g_{||}$ whereas the $g_{\perp}$ value would be 2.07. Then, an average g value of 2.10 was considered as a fixed value in the fitting of magnetic susceptibility data, as described previously.

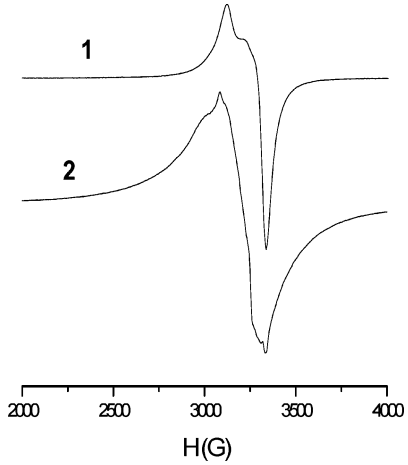

Figure 5. Powder EPR spectra recorded at 4 K for compounds **1** and **2**.

Compound **2** shows a broader band probably arising from the superimposition of different transitions, assignable to either the cationic or the anionic moieties, since both ionic fragments (the cationic binuclear complex and the H-bond interacting counteranions) present a relatively low coupling constant and this makes establishing a difference between both contributions unfeasible.

Acknowledgment. A.K. is grateful to CSIR, New Delhi, India, for a Senior Research Fellowship. This research has been financed by MCYT of Spain through Projects BQU2000-0458, BQ2000/0791, BQ2003/00538, and BQU2003-2884. A.L. is grateful to CIRIT Generalitat de Catalunya (Spain) for the Distinction award and the aid SGR2001-UG-291.

Supporting Information Available: Additional information regarding MO calculations and a CIF file containing all crystallographic information for complex **1** and **2**. This material is available free of charge via the Internet at http://pubs.acs.org.

IC049882J

(26) Desplanches, C.; Ruiz, E.; Álvarez, S. *Chem. Commun.* **2002**, 2614−2615.
(27) Muhonen, H. *Inorg. Chem.* **1986**, *25*, 4692−4698.
(28) (a) Reference 19. (b) Roberts, S. A.; Bloomquist, D. R.; Willett, R. D.; Dodgen, H. W. *J. Am. Chem. Soc.* **1981**, *103*, 2603−2610. (c) Colombo, A.; Menabue, L.; Motori, A.; Pellacani, G. C.; Porzio, W.; Sandrolini, F.; Willett, R. D. *Inorg. Chem.* **1985**, *24*, 2900−2905. (d) Inoue, M.; Kishita, M.; Kubo, M. *Inorg. Chem.* **1967**, *6*, 900−902. (e) Scott, B.; Geiser, U.; Willett, R. D.; Patyal, B.; Landee, C. P.; Greeney, R. E.; Manfredini, T.; Pellacani, G. C.; Corradi, A. B.; Battaglia, L. P. *Inorg. Chem.* **1988**, *27*, 2454−2460. (f) Honda, M.; Katayama, C.; Tanaka, J.; Tanaka, M. *Acta Crystallogr., Sect. C* **1985**, *41*, 197−199.